Available online at www.sciencedirect.com
SCIENCE DIRECT®
Journal of Solid State Chemistry 177 (2004) 4724–4731
JOURNAL OF SOLID STATE CHEMISTRY
www.elsevier.com/locate/jssc

Investigation of the relative stabilities of various allotropic phases of elemental tellurium under pressure and their interconversion paths by electronic structure calculations and crystal structure analyses

C. Soulard[a], X. Rocquefelte[a], M. Evain[a], S. Jobic[a,*], H.-J. Koo[b], M.-H. Whangbo[c,*]

[a]*Institut des Matériaux Jean Rouxel (UMR 6502), Laboratoire de Chimie des Solides, 2 rue de la Houssinière, BP 32229, 44322 Nantes Cedex 3, France*
[b]*Department of Chemistry, Kyung Hee University, Seoul 130-701, South Korea*
[c]*Department of Chemistry, North Carolina State University, Raleigh, NC 27695-8204, USA*

Received 17 May 2004; received in revised form 27 August 2004; accepted 30 August 2004

Abstract

Elemental tellurium adopts a number of different structures under pressure. The relative stabilities of these allotropes and the interconversion between them were examined on the basis of first principles electronic band structure calculations with and without external pressure. The relative stabilities of the allotropes were also analyzed by estimating the overall strength of covalent bonding on the basis of the Te–Te overlap populations determined from tight-binding electronic structure calculations. The crystal structures of the allotropes were analyzed to determine how one form can transform into another form under pressure. Our study leads to the energy profile of tellurium as a function of pressure consistent with experiment, shows that the relative stabilities of the allotropic phases of Te are mainly governed by the overall strength of covalent bonding, and that all the allotropes are intimately related in structure, and one form can be readily converted to another form under pressure via a simple interconversion path.

Keywords: Tellurium; Phase transition; High pressure; Electronic structure

1. Introduction

Elemental tellurium adopts a number of different structures under pressure. The stable form at ambient pressure is the Se-type structure (Te-I) [1], which consists of one-dimensional (1D) helical chains with the coordination number (CN) of two (CN = 2). Tellurium was reported to adopt the As-type structure (Te-I′) at about 1.5 GPa, which has 2D layers made up of puckered Te_6 rings (CN = 3) [2]. At 4.5 GPa tellurium has a monoclinic structure (Te-II) that consists of puckered layers made up of Te_4 rings (CN = 4) [3], and at about 7 GPa the monoclinic structure is converted to an orthorhombic structure (Te-III) that has slightly puckered layers made up of Te_4 rings (CN = 4) [3]. The distinction between these two structures is somewhat arbitrary, because Te-III is deduced from Te-II by a slight, continuous change in the monoclinic angle. At about 10.6 GPa, tellurium adopts the β-Po-type 3D structure (Te-IV) (CN = 6) [4], which is transformed to the body centered cubic (*bcc*) structure (Te-V) (CN = 8) at 27 GPa [5]. The *bcc* structure is a special case of the rhombohedral β-Po cell with the angle of 109.5°. The cell volume per Te decreases in the order Te-I (34.27 Å^3) > Te-I′ (30.76 Å^3) > Te-III (29.89 Å^3) > Te-II (26.49 Å^3) > Te-IV (24.40 Å^3) > Te-V (20.65 Å^3) (at ambient pressure for Te-I, and at 3, 5, 7, 11 and 27 GPa for Te-I′, Te-III, Te-II, Te-IV and Te-V, respectively) [1–5].

*Corresponding author. Fax: +33-2-40-37-39-95.
E-mail address: stephane.jobic@cnrs-imm.fr (S. Jobic).

0022-4596/$ - see front matter © 2004 Elsevier Inc. All rights reserved.
doi:10.1016/j.jssc.2004.08.040

Thus, as empirically expected, a pressure increase shrinks the cell volume and induces an increase in the CN.

The structural motifs that elemental tellurium exhibits are also encountered in tellurides of alkaline, alkaline earth, transition metal and lanthanide elements. For example, the Te chains of Te-I are similar in structure to the linear zigzag fragments $[Te_n]^{2-}$ (i.e., $n = 2-6$) commonly found in the Zintl phases A_xTe_y (A = alkali and alkaline earth elements) [6–13], the As-type layers of Te-I′ remind us of the Te layers found in the ditellurides of late transition metal elements MTe_2 (i.e., M = Pd, Pt) (with short intra- and interlayers Te–Te distances), and the Te layers of Te-III show similarities with those found for $LnTe_2$ phases (Ln = lanthanides) [14,15] (i.e., Te–Te ≈ 3.10 Å in Te-III, 3.04 Å in $LaTe_2$ and 3.20 Å in $CeTe_2$). Consequently, a parallel can be drawn between the structures of these telluride compounds and the allotropes of elemental tellurium.

On the basis of first principles electronic structure calculations, Kirchhoff et al. [16] carried out geometry optimizations for Te-I, Te-III, Te-IV and Te-V as a function of the volume. They found that the Te-I structure is the most stable phase at zero external pressure, that the Te-IV structure has a lower energy than does the Te-III structure, but the energy difference between Te-III and Te-IV lies within the inaccuracy of the calculation. Moreover, a recent experimental study of Takumi et al. [17] suggests that Te-III is stable between 7 and 27 GPa, and a phase transition to Te-IV occurs at 27 GPa, while that of Hejny and McMahon [18] indicates that Te-II and Te-III belong to only one allotropic phase with an incommensurate monoclinic structure and is stable from 4.5 to 29.2 GPa, and the transition from Te-III to Te-IV is absent. Thus, uncertainties and doubts remain concerning the occurrence of some phase transitions, the nature of the exact structure stable under pressure, and the range of stability of some structure types. Consequently, it is important to probe the relative stabilities of various allotropes on the basis of principles electronic structure calculations. It is also interesting to examine possible interconversion paths between the allotropes and hence gain some insight into the microscopic processes that occur under external pressure.

In the present work, we examine the relative stability of the six allotropic phases of elemental Te on the basis of first principles electronic band structure calculations using the Vienna ab initio simulation package (VASP) [19–21] with and without specified external pressures. Then, we examine the charge distribution in the six allotropes of Te on the basis of extended Hückel tight-binding (EHTB) electronic bands structure calculations using the CAESAR code [22,23]. We then analyze the crystal structures of the allotropic phases to investigate their interconversion paths.

2. Electronic structure study of the relative stabilities of the allotropic forms and their interconversion

The cell parameters and the atom positions of the various Te phases were optimized by performing electronic band structure calculations using the VASP code, which is based on the density functional theory within the local-density approximation. The present VASP calculations employed ultrasoft pseudopotentials constructed using the Vanderbilt recipe [24,25], a finite temperature density functional approximation, an optimized mixing routine and a conjugate gradient scheme (Broyden [26] mixing scheme). All calculations were performed using the generalized-gradient approximation as proposed by Perdew and Wang [27]. The integration in the Brillouin zone (BZ) for the semiconducting Te-I and Te-I′ structure types and for the metallic Te-II, Te-III, Te-IV and Te-V structure types were performed with the Monkhorst–Pack [28] k-point meshes $(8 \times 8 \times 6)$, $(8 \times 8 \times 4)$, $(6 \times 2 \times 4)$, $(6 \times 4 \times 8)$, $(6 \times 6 \times 4)$ and $(4 \times 4 \times 4)$, respectively.

To determine the relative stability of the different Te polymorphs, a series of calculations was first carried out at ambient pressure (0.1 MPa) with the initial atomic positions and cell parameters taken from the literature. After convergence, the crystal symmetry operations were examined and the crystal space group was determined with the help of the Endeavour package [29]. The structure of Te-I is well reproduced with less than 4% difference in the volume (i.e., $V = 105.51$ Å^3 instead of 101.82 Å^3). As expected, the cell parameters and the cell volumes are significantly larger for Te-II, Te-III, Te-IV and Te-V than those determined under pressure, although the overall structures are similar. The relative stabilities of the Te phases (based only on our calculations of the internal energies at 0 K and 0 GPa) increase in the order, Te-I′ (−2.144 eV) < Te-V (−2.783 eV) < Te-III (−3.000 eV) < Te-II (−3.014 eV) < Te-IV (−3.113 eV) < Te-I (−3.156 eV), where the numbers in parentheses are the calculated total energies per Te. In our calculations for the Te-I′ structure, it was not possible to retain its structure once geometry relaxation is allowed because it becomes the Te-IV structure. The Te-I′ phase, observed only by Kabalkina et al. [2], is a subject of controversy [4,5].

In a second series of calculations, pressure was taken into account by introducing a stress tensor that allows structure relaxations (i.e., optimizations of the unit cell parameters as well as the atom positions) at a specified external pressure. Only three phases could be observed under these calculations: Te-I at low pressure, Te-IV at intermediate pressures and Te-V beyond 40 GPa. At a given pressure, the Te-I′ structure type may erratically converge toward either the Te-I structure or the Te-IV structure. This shows that there exists an interconnection path between Te-I and Te-IV, and Te-I′ lies on this

pathway. Similarly, calculations carried out for Te-II and Te-III systematically converged to the Te-IV form. Again, this suggests that there exists a pathway between Te-II (and therefore Te-III, *see above*) and Te-IV. Te-II and Te-III could be quasi-stable phases or unstable phases (see Fig. 1). Calculations carried out for Te-IV and Te-V account for the evolution of the structure with a rhombohedral angle ranging from 104.2° to 109.47° for pressure at 20–40 GPa, respectively.

As described above, our calculations suggest strongly that all the allotropes of Te are intimately related, one form with a given structural arrangement converting to another form under pressure. Given the relative energies of the Te phases calculated without external pressure, one might propose the energy profile of tellurium as a function of pressure, as shown in Fig. 1, to explain why Te-I′, Te-II and Te-III are not observed in all pressure experiments.

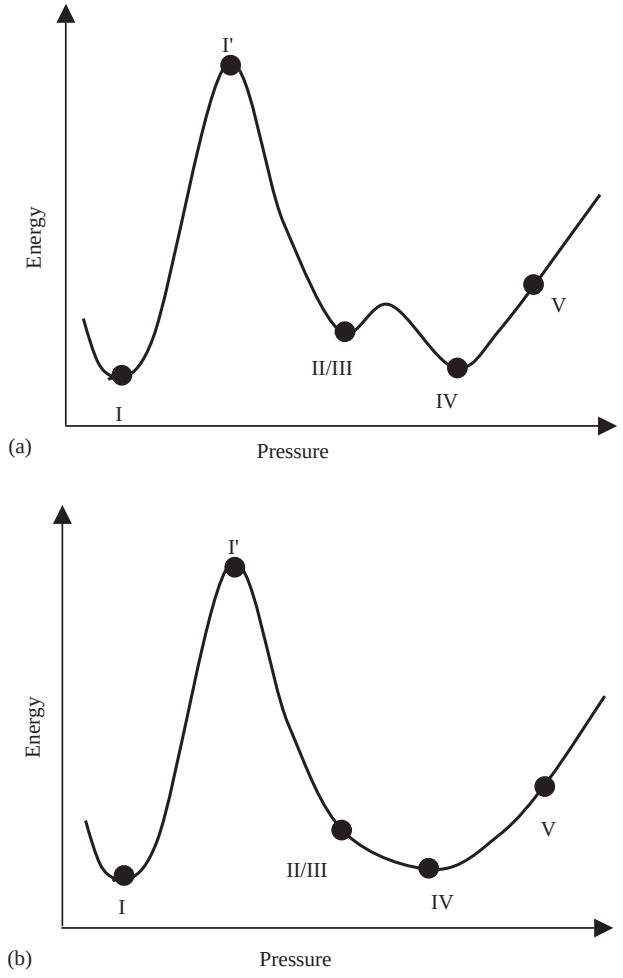

Fig. 1. Schematic energy profiles of elemental tellurium as a function of pressure. When pressure is taken as a reaction coordinate, the Te-I and Te-IV phases are minimum-energy structures, the Te-I′ phase is the transition state between Te-I and Te-IV, and the Te-V phase is a transient structure. The Te-II and Te-III phases are regarded as intermediates in (a), and as transient structures in (b).

3. Analysis of charge distributions of the allotropic forms and their relative stabilities

To examine the charge distributions in the various allotropic forms (I, I′, II, III, IV, V) of Te, EHTB electronic band structure calculations were carried out on the structures reported in the literature. Te-I has a band gap and hence is a semiconductor, while all other allotropes have partially filled bands and hence are predicted to be metallic. These are in agreement with experiment except for Te-I′, which was reported to be a semiconductor [3]. The apparent failure for Te-I′ might be due to the crystal structure of Te-I′ employed for calculations. It was reported that tellurium becomes metallic beyond 4.5 GPa [3], and Te-II becomes a superconductor below 3.3 K [30,31].

To gain insight into the trend in the relative stabilities of the six allotropes of Te, we calculate the overlap populations of their Te–Te bonds (including their short Te⋯Te contacts) on the basis of EHTB electronic band structure calculations. The distances of the Te–Te bonds present in the allotropes are listed in Table 1, where f_i refers to how many times each Te–Te bond type i occurs in a unit cell, and P_i is the overlap population per bond

Table 1
Te–Te overlap populations of various allotropic phases of elemental tellurium obtained by EHTB calculations

Phase	Te–Te (Å)	f_i	P_i	Z	TOPT
I[1]	2.867	3	0.45		
	3.472	6	−0.01		
				3	0.43
I′[2]	2.868	9	0.18		
	3.477	9	0.03		
	4.208	18	−0.05		
				6	0.165
II[3]	2.790	2	0.48		
	3.103/3.104	6	0.09		
	3.417/3.469/3.514/3.573	8	−0.02		
	4.143/4.203/4.257	8	−0.02		
				4	0.295
III[3]	2.680	4	0.29		
	2.992	4	0.15		
	3.541	4	−0.14		
	3.883	4	−0.03		
				4	0.265
IV[4]	2.968	3	0.16		
	3.646/3.669	4	−0.02		
				1	0.40
V[5]	3.339	8	0.09		
	3.856	6	−0.05		
				2	0.21

[a]The number of the bonds with a specific bond length that occur in a unit cell.
[b]The overlap population of the bond with a specific bond length.
[c]The sum of all the overlap populations per Te.

for the Te–Te bond type i. Given the number of Te atoms per unit cell as Z, the overall strength of covalent bonding in each allotrope can be measured by the total overlap population per Te (TOPT) defined as

$$\mathrm{TOPT} = \left(\sum_i f_i P_i\right) \Big/ Z.$$

The values of f_i, P_i, Z and TOPT for each allotrope are summarized in Table 1. In terms of the overall strength of covalent bonding determined by the TOPT values, the stabilities of the six allotropes increase in the order, Te-I′ (0.165) < Te-V (0.210) < Te-III (0.265), Te-II (0.295) < Te-IV (0.400) < Te-I (0.43). Except for the relative stabilities between Te-II and Te-III, this sequence is exactly the same as that found in terms of the total electronic energies determined by first principles electronic band structure calculations. Thus, the overall strength of covalent bonding is a primary factor affecting the relative stabilities of the allotropic phases of Te.

4. Interconversion paths between the allotropic phases

Our discussion of Section 2 indicates that all the allotropes of Te are intimately related in structure, and one form can be readily converted to another form under pressure. Thus, we analyze the crystal structures of the allotropic phases to investigate their interconversion paths. It was noted that on a qualitative level, the Te-I structure can be regarded as arising from a 3D Peierls distortion from a simple cubic structure [32].

From the Se to the As-type structure. As depicted in Fig. 2, the Se-type structure consists of helical Te chains aligned along the c-direction. Each helical Te chain has three atoms per pitch. Fig. 3 shows a projection view of one layer of the As-type structure, and there are three layers per unit cell of the As-type structure. This layer is made up of strongly puckered Te_6 rings with ∠Te–Te–Te = 94.4°. Puckered Te_6 rings with ∠Te–Te–Te close to 90° can be constructed from every four adjacent helical Te chains, as shown in Fig. 4. To form 2D layers, every second Te–Te bond of each helical Te chain should be broken, as depicted in Fig. 5.

From the As type to the monoclinic to the orthorhombic structure. The monoclinic structure consists of puckered layers made up of Te_4 rings (Fig. 6). In Fig. 7a, a puckered layer of Te_6 rings of the As-type structure is viewed in terms of "zigzag" chains. Then a puckered layer of the monoclinic structure (Fig. 7b) is obtained from a layer of the As-type structure by sliding every second "zigzag" chains in opposite directions, as depicted in Fig. 7a. The orthorhombic structure consists of slightly puckered layers made up of Te_4 rings (Fig. 8). The orthorhombic structure can be obtained from the monoclinic structure by reducing the extent of puckering of each layer and then by sliding every second flattened layers in opposite directions.

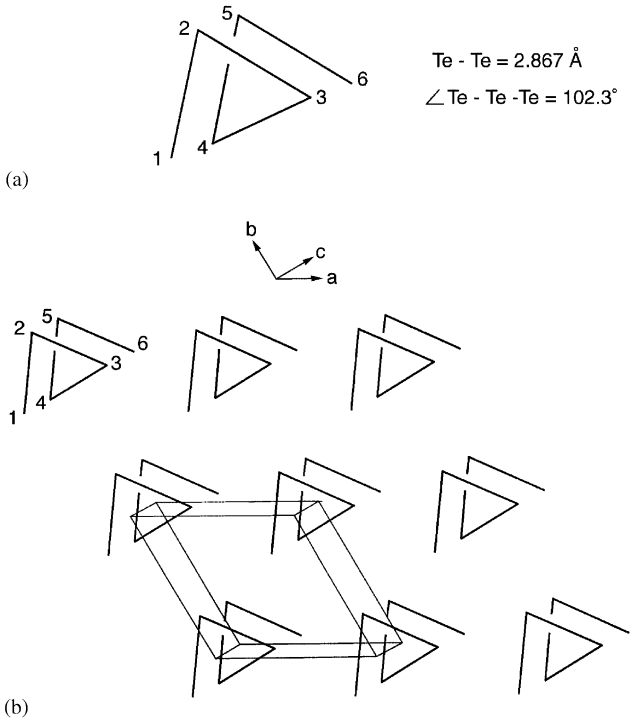

Fig. 2. Se-type structure of tellurium: (a) helical Te chain and (b) arrangement of helical Te chains.

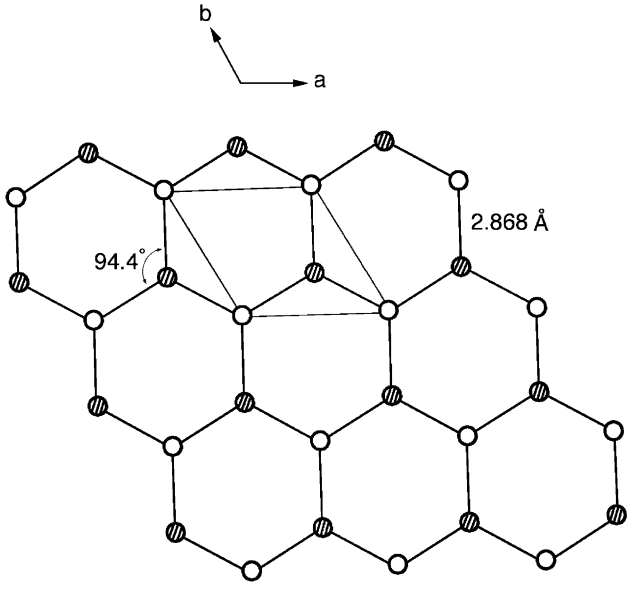

Fig. 3. Projection view of one layer of the As-type structure of tellurium.

From the monoclinic to the β-Po-type structure. As already mentioned in Kirchoff work, the β-Po structure can be obtained from the monoclinic type by decreasing only the interlayer Te–Te distances represented by

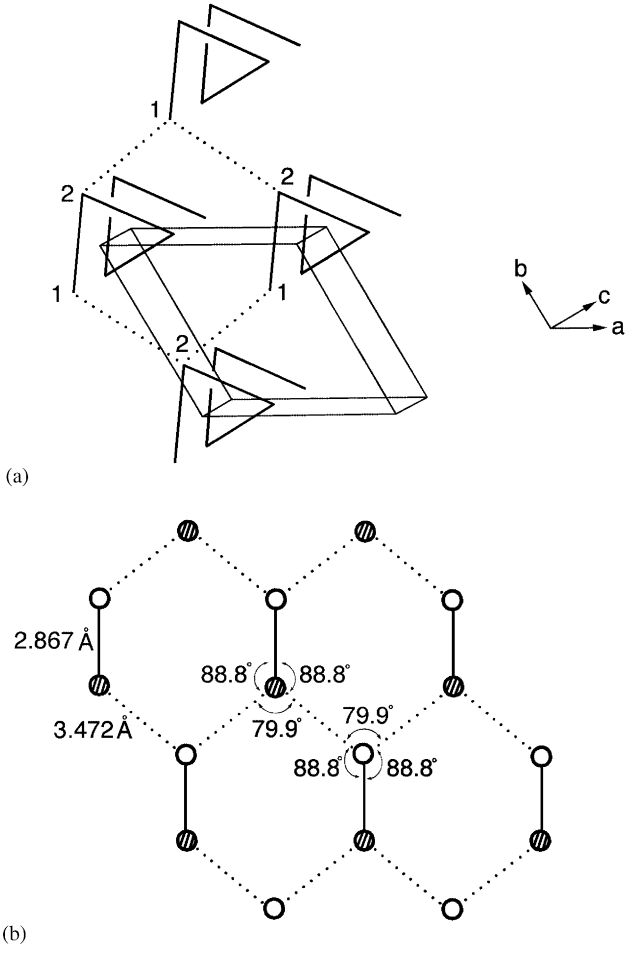

Fig. 4. Construction of a layer of the As-type structure from the helical Te chains of the Se-type structure. (a) Formation of a puckered Te_6 ring from four adjacent helical chains. (b) Single layer made up of puckered Te_6 rings.

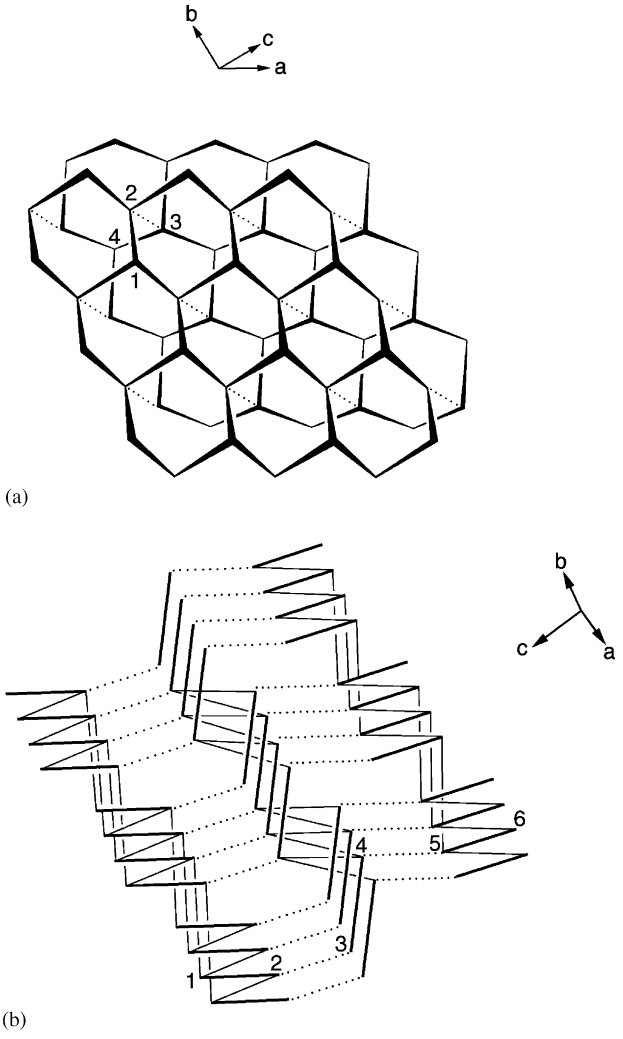

Fig. 5. Puckered layers of the As-type structure constructed from the Se-type structure. (a) Perspective view of two adjacent puckered layers. (b) Perspective view of three puckered layers. The dotted lines are the Te–Te bonds to be broken.

dotted lines in Fig. 8. The β-Po is obtained when the intra- and interlayer distances are equal.

From the Se to the β-Po-type structure. To form the β-Po-type structure from the Se-type structure, each unit cell of the β-Po-type structure can be assembled from four adjacent helical chains as indicated in Figs. 9a and b, where the Te atoms 2, 3′, 4′ and 3‴ form one face, and the atoms 3, 4″, 5 and 4 form the opposite face. The geometrical parameters associated with such a unit cell arising from the Se-type structure are described in Fig. 10.

From the β-Po and Se type to the bcc structure. To consider how the *bcc* structure is derived from the β-Po-type structure, it is convenient to describe the crystal structures of both types in terms of "layers". The *bcc* structure is shown in Fig. 11, where the thick lines are used to indicate "layers", and the thin lines to show the interlayer connections. The β-Po-type structure is shown in Fig. 12, where the thick lines are used to indicate "layers", and the dotted lines to show the interlayer connections. As indicated by arrows in Fig. 12, the *bcc*-type structure can be obtained from the Hg-type structure by sliding every second layers in opposite directions. On a more simple way, the cubic structure can be obtained from the rhombohedric structure by simply increasing the α angle from 103.3° to 109.47° (the calculations reproduced this evolution very well). In a similar manner, as shown in Fig. 13, the Se-type structure can also be described in terms of layers and the *bcc* structure can be obtained from the Se-type structure by sliding every second layers in opposite directions.

5. Concluding remarks

The cell parameters and the atom positions of the various allotropes of Te were examined on the basis of

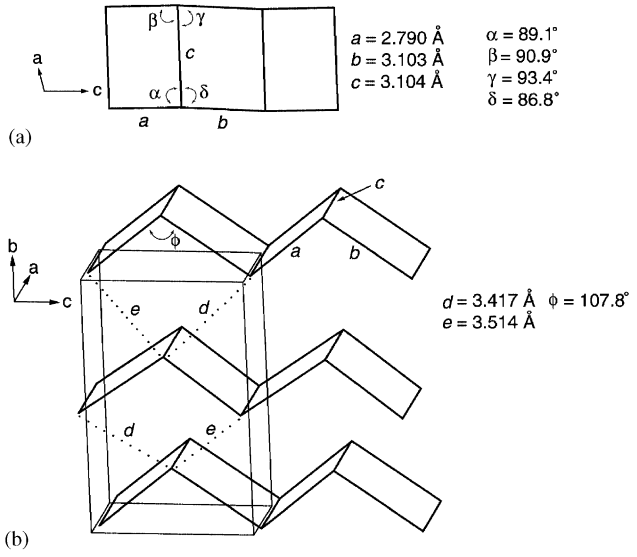

Fig. 6. Geometrical parameters of the layers of the monoclinic-type structure.

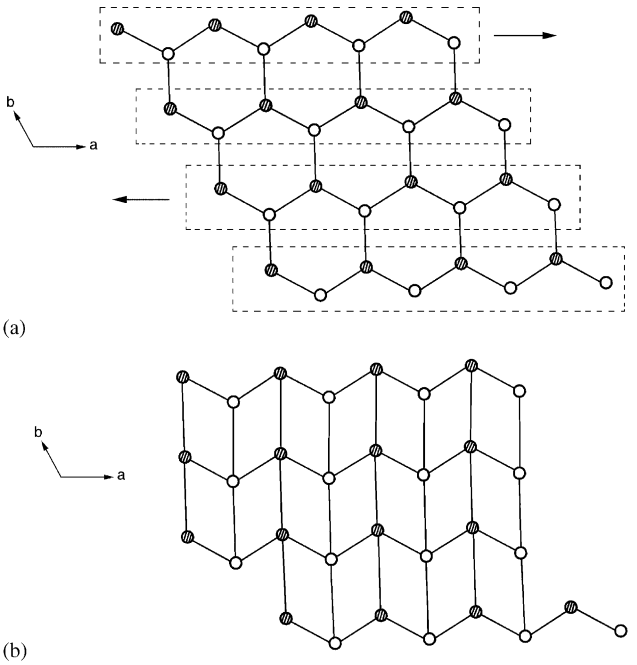

Fig. 7. Formation of a layer of the monoclinic-type structure from a layer of the As-type structure by sliding every second "zigzag" chains in opposite directions.

first principles VASP electronic structure calculations with and without external pressure. Our calculations without external pressure well reproduce the structure of Te-I, and show larger cell volumes for Te-II, Te-III, Te-IV and Te-V than those determined under pressure, as expected. The relative stabilities of the Te phases are calculated to increase in the order, Te-I′ < Te-V < Te-III < Te-II < Te-IV < Te-I. Our calculations with external

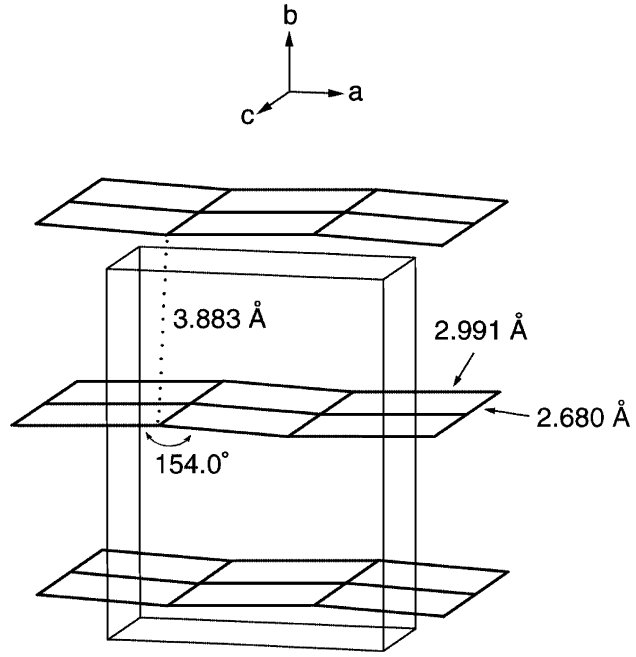

Fig. 8. Geometrical parameters of the layers of the orthorhombic-type structure.

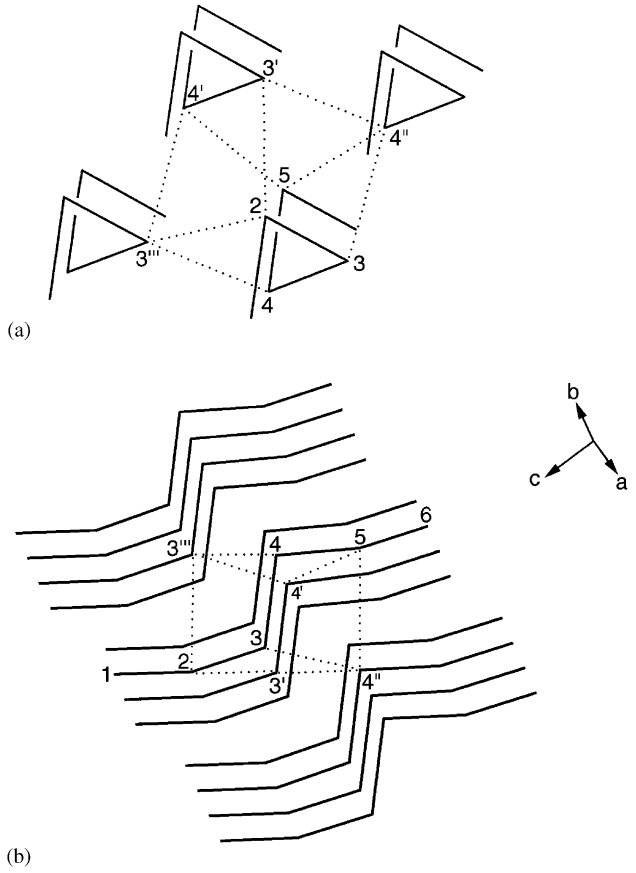

Fig. 9. Two perspective views of the construction of a unit cell of the Hg-type structure from the four adjacent helical Te chains of the Se-type structure. (a) A view approximately along the chain direction. (b) A view approximately perpendicular to the chain direction.

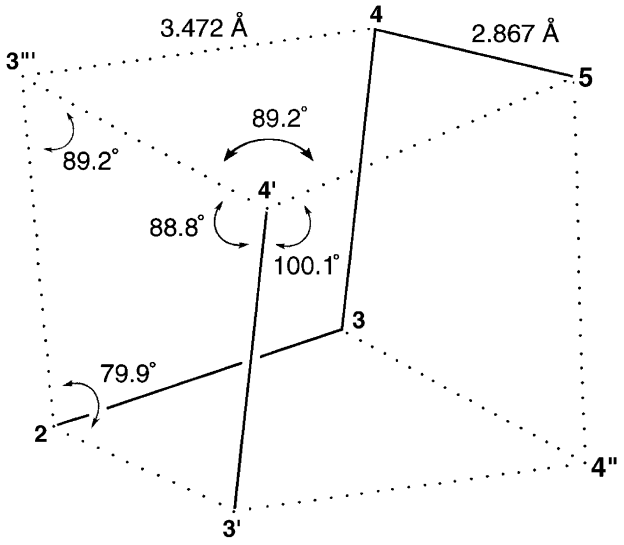

Fig. 10. Geometrical parameters associated with a cell of the Se-type structure leading to the Hg-type structure.

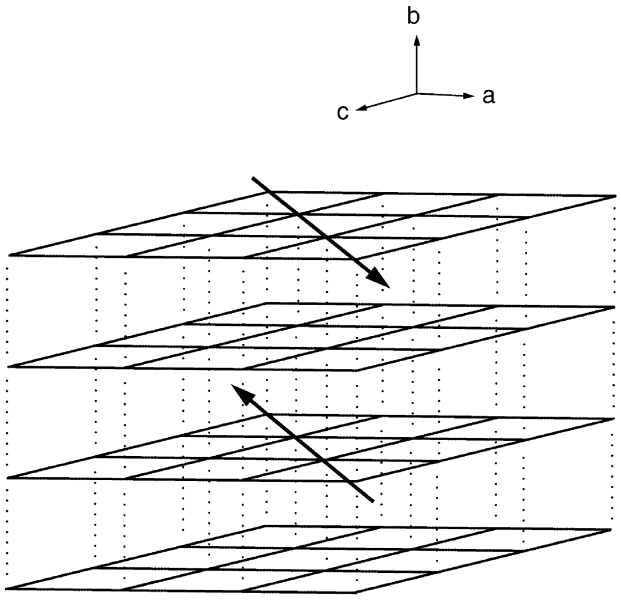

Fig. 12. "Layer" view of the Hg-type structure. The thick lines are used to indicate "layers", and the dotted lines to show the interlayer connections. The *bcc*-type structure is obtained by sliding every second layers in opposite directions as indicated.

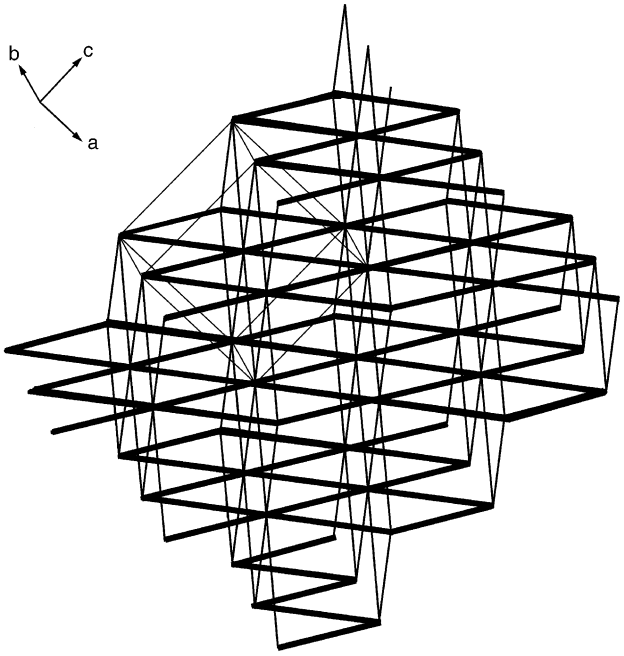

Fig. 11. "Layer" view of the *bcc*-type structure. The thick lines are used to indicate "layers", and the thin lines to show the interlayer connections. A unit cell box is also shown.

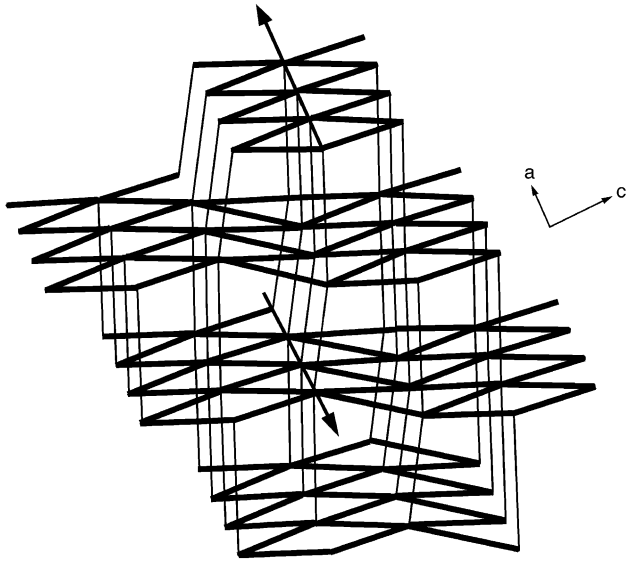

Fig. 13. "Layer" view of the Se-type structure. The thick lines are used to indicate "layers", and the thin lines to show the interlayer connections. The *bcc*-type structure is obtained by sliding every second layers in opposite directions as indicated.

pressure reproduce Te-I structure at low pressure, the Te-IV at intermediate pressures and Te-V beyond 40 GPa. In addition, they show that the Te-I′ is converted to either Te-I or Te-IV, and Te-II and Te-III to Te-IV. Thus, the energy profile of tellurium as a function of pressure is summarized as in Fig. 1, which depicts that Te-I is the global-minimum-energy phase, Te-IV is a local-minimum-energy structure, Te-I′ is a transition state structure, Te-II and Te-III are either intermediate or transient states, and Te-V is a transient state. In terms of the Te–Te overlap populations obtained from EHTB calculations, we estimated the overall strength of covalent bonding in the allotropes of Te. According to this analysis, the stabilities of the allotropes increase in the order, Te-I′ < Te-V < Te-III,

Te-II < Te-IV < Te-I, in good agreement with the relative stabilities determined from first principles electronic structure calculations, thereby showing that the relative stabilities of the allotropic phases of Te are governed by the overall strength of covalent bonding. Te-I is the most stable form of Te because its antibonding levels are unoccupied unlike in other Te phases with coordination number higher than two. In agreement with the theoretical and experimental observations, our analysis of the crystal structures of the allotropes indicates that all the allotropes are intimately related in structure, and one form can be readily converted to another form under pressure via a simple interconversion path.

Acknowledgments

The work at NCSU was supported by the Office of Basic Energy Sciences, Division of Materials Sciences, US Department of Energy, Under Grant DE-FG02-86ER45259.

References

[1] C. Adenis, V. Langer, O. Lindqvist, Acta Crystallogr. C 45 (1989) 941.
[2] [a] S.S. Kabalkina, L.F. Vereshchagin, B.M. Shulenin, J. Exp. Theor. Phys. 45 (1963) 2073;
[b] S.S. Kabalkina, L.F. Vereshchagin, B.M. Shulenin, Sov. Phys. JETP 18 (1964) 1422.
[3] K. Aoki, O. Shimomura, S. Minomura, J. Phys. Soc. Jpn. 48 (1980) 551.
[4] J.C. Jamieson, D.B. McWhan, J. Chem. Phys. 43 (1965) 1149.
[5] G. Parthasarathy, W.B. Holzapfel, Phys. Rev. B 37 (1988) 8499.
[6] P. Böttcher, Angew. Chem. Int. Ed. Engl. 27 (1988) 759.
[7] D.Y. Valentine, O.B. Cavin, H.L. Yakel, Acta Crystallogr. B 33 (1977) 1389.
[8] W.S. Sheldrick, B. Schaaf, Z. Naturforsch. B 49 (1994) 993.
[9] D.M. Smith, J.A. Ibers, Coord. Chem. Rev. 200 (2000) 187.
[10] P. Böttcher, R. Keller, J. Less-Common Met. 109 (1985) 311.
[11] W.S. Sheldrick, M. Wachhold, Angew. Chem. Int. Ed. Engl. 34 (1995) 450.
[12] Q. Liu, N. Goldberg, R. Hoffmann, Chem. Eur. J. 2 (1996) 390.
[13] P. Böttcher, U. Kretshmann, J. Less-Common Met. 95 (1983) 81.
[14] K. Stoewe, J. Solid State Chem. 149 (2000) 155.
[15] W.B. Pearson, Z. Kristallogr. 171 (1985) 23.
[16] F. Kirchhoff, N. Binggeli, G. Galli, S. Massidda, Phys. Rev. B 50 (1994) 9063.
[17] M. Takumi, T. Masamitsu, K. Nagata, J. Phys.: Condens. Matter 14 (2002) 10609.
[18] C. Hejny, M.I. McMahon, Phys. Rev. Lett. 91 (2003) 215502.
[19] G. Kresse, J. Furthmuller, Vienna ab-initio Simulation Package (VASP), Institut für Materialphysik, Universität Wien, Austria. See also: http://cms.mpi.univie.ac.at/VASP/.
[20] G. Kresse, J. Furthmuller, Comput. Sci. 6 (1996) 15.
[21] G. Kresse, J. Furthmuller, Phys. Rev. B 54 (1996) 11169.
[22] M.-H. Whangbo, R. Hoffmann, J. Am. Chem. Soc. 100 (1978) 6093.
[23] J. Ren, W. Liang, M.-H. Whangbo, Crystal and electronic structure analysis using CAESAR, 1998, http://chvamw.chem.ncsu.edu/.
[24] G. Kresse, J. Hafner, J. Phys.: Condens. Matter 6 (1994) 8245.
[25] D. Vanderbilt, Phys. Rev. B 41 (1991) 7892.
[26] C.G. Broyden, Math. Comput. 19 (1965) 577.
[27] J.P. Perdew, Y.Y. Wang, Phys. Rev. B 33 (1986) 8800.
[28] H.J. Monkhorst, J.D. Pack, Phys. Rev. B 13 (1976) 5188.
[29] H. Putz, J.C. Schoen, M. Jansen, J. Appl. Crystallogr. 32 (1999) 864.
[30] B.T. Matthias, J.L. Olsen, Phys. Lett. 13 (1964) 202.
[31] Y. Akahama, M. Kobayashi, H. Kawamura, Solid State Commun. 84 (1992) 803.
[32] A. Decker, G.A. Landrum, R. Dronkowski, Z. Anorg. Allg. Chem. 628 (2002) 295.